Spherical voids and clusters in the stabilized jellium model: self-consistent Kohn-Sham calculations

1993 J. Phys.: Condens. Matter 5 9049

(http://iopscience.iop.org/0953-8984/5/49/007)

J. Phys.: Condens. Matter 5 (1993) 9049–9058. Printed in the UK

Spherical voids and clusters in the stabilized jellium model: self-consistent Kohn–Sham calculations

P Ziesche†, M J Puska, T Korhonen and R M Nieminen
Laboratory of Physics, Helsinki University of Technology, 02150 Espoo, Finland

Received 13 May 1993, in final form 8 September 1993

Abstract. The void formation energies in simple metals are calculated in the stabilized jellium model. The total energies of stabilized jellium spheres mimicking small clusters of simple metals are determined. The electronic structures are solved in both cases self-consistently within the local density approximation for electron exchange and correlation. The planar surface energies and the curvature energies are extracted from the results. The stabilized jellium model is shown to give a physically meaningful description of planar surfaces as well as surfaces with positive or negative curvature. The results for voids and clusters are discussed using the so-called liquid drop model and its generalization. They are used to estimate edge and step formation energies.

1. Introduction

The jellium model, applicable to simple sp-bonded metals, has had an important role in the development of theoretical surface physics [1–3]. It has also increased our understanding of the properties of vacancies and voids in bulk crystals [4–6]. Recently, interest in surface physics has shifted to more complex structures such as steps or adatom or vacancy islands on surfaces (see [7] and references therein) and phenomena such as surface roughening (see [8] and references therein) or faceting of finite surfaces. The ability of the jellium model to provide insights into this kind of problem should be investigated.

The simple jellium model has, however, the deficiency that jellium is stable only at one density. This is intrinsically related to the unphysical negative surface and void formation energies at high jellium densities [1,4]. This deficiency has been corrected from early works by re-introducing the ions using pseudopotentials and perturbation theory [1,6], or variationally [2,6]. Very recently, Perdew and co-workers [9], as well as Shore and Rose [10], introduced the so-called 'structureless pseudopotential' or 'stabilized jellium' model, which rectifies the drawbacks of the jellium model in an attractively simple manner.

The stabilized jellium model has been shown to reproduce quite reasonably the surface energies of the simple metals [9–11]. The model has also been applied to void formation energies by Fiolhais and Perdew [12] and by Perdew and co-workers [13]. It is shown in these works that the model gives reasonable values for the vacancy formation energies for alkali metals and for Al. However, the calculation by Perdew and co-workers [13] is not based on self-consistent electron structure calculations for spherical voids, but on a Padé approximation linking the small- and large-void radius regions. The large-void radius limit is treated in the liquid drop model [14], in which the parameters are the surface energy and

† Permanent address: Many-Body Problems Group, PO Box 410113, D-01224 Dresden, Federal Republic of Germany.

0953-8984/93/499049+10$07.50

the so-called curvature energy. For the small-void radius limit Perdew and co-workers use perturbation and linear response theory, giving the expansion coefficients rigorously for the vanishing void radius.

The purpose of this work is to calculate self-consistently the electronic structures and total energies of voids in the stabilized jellium model. We use density functional theory within the local density approximation (LDA) for electron exchange and correlation [15] and solve numerically the ensuing Kohn–Sham equations. The self-consistent void formation energies obtained put the conclusions by Perdew and co-workers [13] on a firmer basis. Moreover, we extend the calculations to stabilized jellium spheres mimicking metal atom clusters. Previous self-consistent approaches [16] have used the unstabilized jellium and therefore the surface contribution to the total energy is unreliable. In this work we show the feasibility of using the stabilized jellium model for the surface energy of clusters. The comparison of the total energies of these spheres with the liquid drop model predictions is also interesting, due to the fact that the curvatures are now positive.

In this work we obtain self-consistent values for the coefficients of the liquid drop model and for the Padé approximation. These coefficients, for example the planar surface energy and the curvature energy, are needed in estimating the energies of complex surface structures. As an application we consider the formation energy of a step on the Al(111) surface.

The organization of this paper is as follows. In section 2 we describe the practical features of the stabilized jellium model important for our applications. In section 3 the results for void and cluster surface energies are presented and discussed. Section 4 contains the application to the step on the Al(111) surface and section 5 is devoted to conclusions.

2. Model

In the stabilized jellium model, the spherical positive background profiles for voids (n_+^{v}) and spheres (n_+^{c}) are

$$n_+^{\mathrm{v}}(r) = \bar{n}\theta(r - R) \tag{1}$$

and

$$n_+^{\mathrm{c}}(r) = \bar{n}\theta(R - r) \tag{2}$$

where $\bar{n} = 3/(4\pi r_s^3)$ is the equilibrium bulk valence electron density, $\theta(r)$ is the usual Heaviside step function, and R is the radius of the void or the jellium sphere. In these and following equations atomic units ($\hbar/me^2 = a_{\mathrm{B}}$ and $me^4/\hbar^2$) are used for the length and the energy, respectively. We consider only neutral jellium spheres, so that the electron number $\frac{4}{3}\pi R^3\bar{n}$ must be an integer and the possible sphere radii for a given density $\bar{n}$ are limited to certain values. For voids in jellium the sphere radius can be a continuous quantity due to the infinite extent of the system.

The stabilization correction adds to the effective potentials for voids ($V_{\mathrm{eff}}^{\mathrm{v}}$) and spheres ($V_{\mathrm{eff}}^{\mathrm{c}}$) the terms

$$\Delta V_{\mathrm{eff}}^{\mathrm{v}}(r) = +\bar{n}\frac{\mathrm{d}\epsilon}{\mathrm{d}\bar{n}}\theta(R - r) \tag{3}$$

and

$$\Delta V_{\mathrm{eff}}^{\mathrm{c}}(r) = -\bar{n}\frac{\mathrm{d}\epsilon}{\mathrm{d}\bar{n}}\theta(R - r) \tag{4}$$

where $\epsilon = t_0 + \epsilon_{xc}$ is the bulk energy per particle in a homogeneous electron gas, containing kinetic energy ($t_0 = \frac{3}{10}k_F^2 = \frac{3}{10}(3\pi^2\bar{n})^{2/3}$) and exchange and correlation energy (ϵ_{xc}) contributions.

The positive background charge distribution and the stabilization correction determine the Kohn–Sham equations to be solved. For simplicity, we use spherical electron densities and the spin-independent LDA formalism (with identical spin-up and spin-down occupancies) for all spheres with open electron shells (while in [17] self-consistent calculations of small stabilized-jellium spheres are based on the local spin-density formalism).

The density-functional total energy for a void can be used to calculate the void formation energy E_R^v. The equation needed in practice is the same as in the jellium model given in [6]. We define the void surface energy per unit area σ_R^v as

$$\sigma_R^v = \frac{E_R^v}{4\pi R^2}. \tag{5}$$

We also calculate the total energy E_R^c for a stabilized jellium sphere and then define the surface energy σ_R^c per unit area for a sphere as

$$\sigma_R^c = \frac{E_R^c - (4\pi/3)R^3\bar{n}(\epsilon + \Delta\epsilon)}{4\pi R^2}. \tag{6}$$

Above, the term subtracted from the total energy is the bulk energy of stabilized jellium corresponding to the volume of the sphere with radius R; $\Delta\epsilon = -\frac{3}{5}(z^{2/3}/r_s) - \bar{n}\,d\epsilon/d\bar{n}$ is the stabilization correction of the bulk energy, and z is the number of valence electrons per atom. For the details about the stabilization correction see [9].

3. Void and cluster surface energies

First we consider voids and stabilized jellium spheres with $R = r_0 = z^{1/3}r_s$, i.e. the Wigner–Seitz radius. Thereby we obtain the monovacancy formation energies $E_{r_0}^v = 4\pi r_0^2\sigma_{r_0}^v$ and the cohesive energies $4\pi r_0^2\sigma_{r_0}^c$. In this model the cohesive energy is the energy per sphere needed to split the infinite stabilized jellium into non-interacting Wigner–Seitz spheres. This energy is the total surface energy of one Wigner–Seitz sphere, and it is determined in this work by a self-consistent calculation for an isolated stabilized jellium sphere. Perdew and co-workers [14] showed, using the semiempirical liquid drop model, that this surface energy explains the cohesive energies of monovalent metals.

The results for vacancy formation energies and cohesive energies corresponding to the r_s and z parameters for several simple metals are collected in table 1 and compared with experimental values. The agreement is surprisingly good for the monovalent alkali metals and also quite fair for the trivalent Al. The calculated vacancy formation energies for the divalent earth-alkaline metals are reasonable in comparison with the available experimental values, but the calculated cohesive energies are too small. This reflects the fact that stabilized jellium spheres with two electrons have a very stable closed shell structure with a relatively low total energy, which leads to a small surface energy. The real earth-alkaline metal atoms also have closed shell structures, but in the atoms the valence electron states have to be orthogonal against the core electrons. This decreases the stability of the free atoms and shifts valence charge out of the core region to the bond region of the metal. Both of these effects increase the cohesive energy of the real metal relative to our model. It is interesting to note that the semiempirical liquid drop model of Perdew and co-workers [14] gives, due

to the absence of the shell effects, cohesive energies that are much too large for divalent metals. The vacancy formation energies and the cohesive energies calculated in the Padé approximation [13, 19, 20] are also shown in table 1. The vacancy formation energies are in a good agreement with our self-consistent values, whereas for the cohesive energy the discrepancies are larger.

Table 1. Monovacancy formation energies and cohesive energies per atom. $4\pi r_0^2\sigma_{r_0}^{v}$ and $4\pi r_0^2\sigma_{r_0}^{c}$ are the present theoretical values, whereas E_{1v}^{f} (taken by [6]) and E_{coh} [18] are the corresponding experimental values. The results of the Padé approximation [13, 19, 20] are shown in parentheses. All energies are in eV.

Metal (z, r_s)	$4\pi r_0^2\sigma_{r_0}^{v}$	E_{1v}^{f}	$4\pi r_0^2\sigma_{r_0}^{c}$	E_{coh}
Li (1, 3.24)	0.37(0.37)	0.37	1.50(1.03)	1.63
Na (1, 3.93)	0.34 (0.33)	0.41	1.19(0.82)	1.11
K (1, 4.86)	0.29(0.28)	0.39	0.89(0.66)	0.93
Rb (1, 5.20)	0.27(0.27)	0.27	0.82(0.59)	0.85
Cs (1, 5.62)	0.26 (0.24)	0.28	0.74(0.54)	0.80
Zn (2, 2.30)	0.74(0.77)	—	1.19(2.18)	1.35
Mg (2, 2.65)	0.75(0.76)	0.84	1.16(1.87)	1.51
Ca (2, 3.27)	0.70(0.69)	0.54	1.04(1.51)	1.84
Sr (2, 3.57)	0.67(0.66)	—	0.98(1.36)	1.72
Ba (2, 3.71)	0.65(0.64)	—	0.95(1.30)	1.90
Al (3, 2.07)	1.02(1.06)	0.67	3.96(3.02)	3.39
Pb (4, 2.30)	1.37(1.39)	0.52	4.57(3.16)	2.03

Table 2. Planar surface energy σ (meV a_B^{-2}) and curvature energy γ (meV a_B^{-1}) according to [13] and [11] and figure 1. The results of [13] arise from the approach of [12].

	σ			γ	
Metal (r_s)	Reference [13]	Reference [11]	Present work	Reference [13]	Present work
Al (2.07)	16.19	16.17	16.15	49.8	44.5
Na (3.93)	3.13	3.15[a]	3.14	9.84	9.54
Cs (5.62)	1.03	1.05	1.055	3.67	3.84

[a] Recalculated for $r_s = 3.93$ from the value 3.01 given in [11] for $r_s = 3.99$.

The void surface energies per unit area corresponding to the valence electron densities in Al, Na, and Cs are shown in figure 1 as a function of the inverse of the void radius. The circles denote the results of the self-consistent calculations and the straight lines correspond to the two first terms of the large-R fit

$$\sigma^{v}(R) = \sigma - \frac{\gamma}{2R} + \mathcal{O}(1/R^2). \tag{7}$$

Above, σ and γ are the planar surface energy and the curvature energy, respectively. Note that we use here the argument R in parenthesis instead of the subscript R to distinguish the continuously fitted functions from the discrete calculated data. In the equations below this convention is also used for N denoting the number of vacancies or atoms. In the liquid drop model [14] only the first two terms of the expansion are considered. The values of the parameters σ and γ obtained in this work for Al, Na, and Cs are given in table 2. There

the planar surface energies σ are compared with self-consistent results [11, 13] obtained using a computer code for the semi-infinite stabilized jellium. Our extrapolations (figure 1) are in good agreement with these. The small differences are probably of numerical origin. The present self-consistent curvature energies γ are also compared with the results obtained in [13] by employing the fourth-order gradient expansion for the kinetic energy [12]. Due to the different approaches used in the present work and in [12, 13] the values for γ are somewhat different and this difference changes sign when the density of the stabilized jellium decreases.

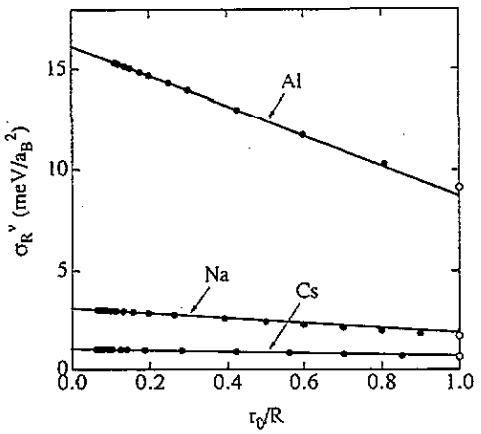

Figure 1. Void surface energy σ_R^v against r_0/R for $r_0 = 2.99$ (Al), 3.93 (Na) and 5.62 (Cs). The full circles denote the results of the self-consistent calculations and the straight lines correspond to linear large-R fits. The open circles correspond to monovacancies.

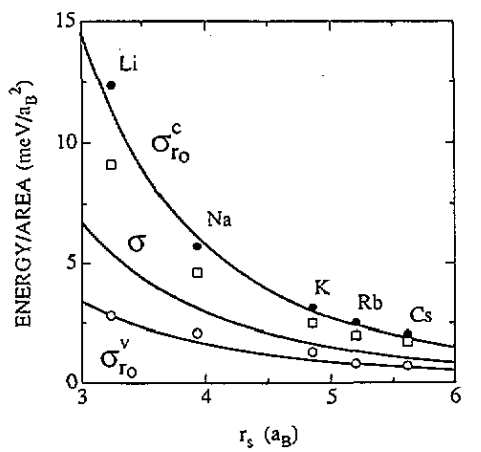

Figure 2. Surface energies of monovacancies, planar surfaces and single 'atoms' of stabilized jellium. The open and full circles correspond to experimental vacancy formation [6] and cohesive [18] energies, respectively. The open squares are the experimental planar surface energies of molten alkali metals extrapolated to zero temperature [21].

Figure 2 shows the surface energies per unit area for the planar surface, for the $z = 1$ monovacancy, and a single 'atom' (the sphere with $R = r_0$) of stabilized jellium as a function of the density parameter r_s. The curves are compared with experimental points for vacancy formation† and cohesive energies [18] of alkali metals. Moreover, the experimental planar surface energies [21] of molten alkali metals extrapolated to zero temperature are also shown. Note that $\sigma^{v}_{r_0} < \sigma < \sigma^{c}_{r_0}$, reflecting the change of the curvature energy from positive to negative when the surface changes from convex to concave. For a real lattice this means that the number of broken bonds decreases. The theoretical and experimental vacancy formation and cohesive energies are in good agreement, but the theoretical planar surface energy curve lies remarkably below the experimental values. This discrepancy has been explained to arise mainly from the increase of the surface energy due to atomic scale corrugations [9, 11].

We note from figure 2 that the planar surface energy curve is closer to the curve corresponding to the vacancy formation energy than that for the cohesive energy, i.e. $(\sigma^{c}_{r_0} + \sigma^{v}_{r_0})/2 > \sigma$. This means that extracting a sphere with radius r_0 from stabilized jellium and leaving a hole behind costs, in addition to the energy due to the increased surface area, a curvature contribution of $4\pi r_0^2(\sigma^{c}_{r_0} + \sigma^{v}_{r_0} - 2\sigma) > 0$.

Our data for the larger voids and spheres can be analysed in terms of the void binding energy per vacancy and the cluster binding energy per atom. Thus, we consider a spherical vacancy cluster of radius $R_N = N^{1/3}r_0$ and having formation energy $4\pi R_N^2\sigma^{v}_{R_N}$, to arise from N single monovacancies each having the formation energy $4\pi r_0^2\sigma^{v}_{r_0}$. The void binding energy per vacancy is then

$$\Delta^{v}_{N} = \frac{1}{N}\left(4\pi R_N^2\sigma^{v}_{R_N} - N4\pi r_0^2\sigma^{v}_{r_0}\right). \tag{8}$$

This quantity vanishes by definition for $N = 1$ ($R_1 = r_0$). For $N \to \infty$ it approaches $-4\pi r_0^2\sigma^{v}_{r_0}$, the negative of the vacancy formation energy, because at this limit $\sigma^{v}_{R_N} \to \sigma$ and $R_N^2/N \to 0$. Similarly, we define the cluster binding energy per atom as

$$\Delta^{c}_{N} = \frac{1}{N}\left(E^{c}_{R_N} - NE^{c}_{r_0}\right) = \frac{1}{N}\left(4\pi R_N^2\sigma^{c}_{R_N} - N4\pi r_0^2\sigma^{c}_{r_0}\right). \tag{9}$$

The latter equality is due to the cancellation of the bulk energy terms, as in the case of the cohesive energy above. The cluster binding energy also vanishes for $N=1$, and for $N \to \infty$ it approaches $-4\pi r_0^2\sigma^{c}_{r_0}$, the negative of the cohesive energy.

The void binding energy per vacancy and the cluster binding energy per atom for stabilized jellium with $r_s = 3.93$ (Na) are plotted in figure 3 as a function of $N^{-1/3}$. In the figure the vacancy formation energy and the cohesive energy are found from the vertical axis on the left. We show results for all clusters between $N=1$ and $N = 20$ and thereafter only for closed shell clusters up to $N = 306$. The full squares and circles correspond to open and closed shell clusters, respectively. The cluster data show oscillations as a consequence of the shell structure, but their relative importance in the total binding energy decreases when the cluster size increases.

The broken and full curves in figure 3 are based on the different fits to the void data. For example, if we use the liquid drop model, i.e. equation (7), the void binding energy per vacancy in (8) becomes

$$\Delta^{v}(N) = -4\pi r_0^2\sigma^{v}_{r_0} + \frac{4\pi r_0^2}{N^{1/3}}\sigma - \frac{2\pi r_0}{N^{2/3}}\gamma + \mathcal{O}(1/R^2). \tag{10}$$

† The experimental data for vacancy formation energies are taken from [6].

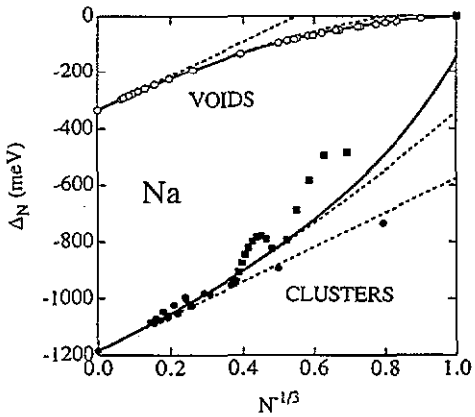

Figure 3. Void binding energy per vacancy (Δ_N^v in (8)) and cluster binding energy per 'atom' (Δ_N^c in (9)) in the stabilized jellium model. N is the number of vacancies or 'atoms', respectively. Open circles correspond to voids. Full circles and squares refer to closed shell and open shell spheres, respectively. The broken lines are obtained with terms up to the planar surface energy in (10) and (11), whereas for the broken curves the curvature contributions are included. The full curves correspond to the generalized liquid drop model of (13).

The corresponding cluster binding energy per atom is then obtained by using the cohesive energy instead of the vacancy formation energy and changing the sign of the curvature (or the curvature energy), i.e.

$$\Delta^c(N) = -4\pi r_0^2 \sigma_{r_0}^c + \frac{4\pi r_0^2}{N^{1/3}}\sigma + \frac{2\pi r_0}{N^{2/3}}\gamma + \mathcal{O}(1/R^2). \tag{11}$$

The broken curves in figure 3 are obtained using these equations whereas the broken lines correspond to the first two terms, the vacancy formation energy or the cohesive energy and the surface energy. Firstly, we see that the cluster data approach the straight line at the largest cluster sizes calculated, the slope of which is determined by the planar surface energy σ. Secondly, the liquid drop model of (10) is quite accurate for the voids. Even in the case of a monovacancy it causes an error of only about 10%. On the other hand, when applied for clusters the relative deviation from the exact results for a given N is larger than in the case of voids. If the liquid drop model of (10) is used to estimate the cohesive energy $4\pi r_0^2 \sigma_{r_0}^c$, the error is about 30%.

It is possible to improve the simple liquid drop model of (7) by using more fitting parameters. For example, one can extend (7) to

$$\sigma^v(R) = \sigma - \frac{\gamma}{2R} + \frac{\delta}{4\pi R^2} + \mathcal{O}(1/R^3) \tag{12}$$

(the extended liquid drop model). The determination of the parameter δ is numerically much more difficult than that of the parameters σ and γ. According to our estimations δ is about 9, -45 and -40 meV for Al, Na and Cs, respectively. The physical meaning of δ is that it describes the interactions between the different parts of the curved surface. Because δ changes sign between Al and Na, this interaction seems to have a different type of character for the high and low electron density systems. If a term corresponding to the third term on the right-hand side of (12) is added to the cluster binding energy per atom in (11) the changes are very small.

In the generalized liquid drop model proposed in [13] the void surface energy is given by the Padé approximation as

$$\sigma^{v}(R) = \frac{\sigma}{1 + (B_1/R) + (B_2/R^2) + (B_3/R^3)}. \tag{13}$$

The corresponding approximation $\sigma^{c}(R)$ for the cluster surface energy is then obtained by analytic continuation, i.e. by making the substitution $R \to -R$. We have used the above form with the values of σ and $B_1 = \gamma/2\sigma$ (table 2) obtained by the large-R fits and then used all the data up to monovacancies to determine B_2 and B_3. The values of the parameters for B_1, B_2 and B_3 are given in table 3 for Al, Na and Cs. The values for B_2 and B_3 differ remarkably from those in [13]. It is evident that the differences in B_2 and B_3 largely cancel in the calculation of the void surface energies. The full curves in figure 3 correspond to the generalized liquid drop model. The approximation joins smoothly the void results and in the case of clusters it predicts the cohesive energy obtained from the calculation for the Wigner–Seitz sphere to within 10%. In the case of Cs the generalized liquid drop model with the present parameters also predicts the cohesive energy well, but for Al the agreement is less satisfactory. This may be partly due to the insufficient accuracy with which we can obtain the B_2 and B_3 parameters in fitting the void energies.

Table 3. Parameters of the Padé fits (13) to the calculated void surface energies. The results of [13] are shown in parentheses.

Metal	B_1 (a_B)	B_2 (a_B^2)	B_3 (a_B^3)
Al	1.38 (1.54)	2.09 (1.39)	2.14 (1.09)
Na	1.52 (1.57)	3.11 (4.42)	13.77 (8.88)
Cs	1.82 (1.78)	1.98 (7.06)	43.83 (25.55)

4. Edges and steps on surfaces

As an application of our results we discuss the total energy characteristics of edges and steps on otherwise planar surfaces using the generalized liquid drop model similarly to [13]. The formation energy of an edge is the difference between the total surface energy for a surface with the edge and the energy of the planar surface with equal area. The former can be calculated using the local curvature $\mathcal{R}^{-1} = \frac{1}{2}(\mathcal{R}_1^{-1} + \mathcal{R}_2^{-1})$, where $\mathcal{R}_1$ and $\mathcal{R}_2$ are the principal curvature radii. We define the curvature-dependent surface energy $\sigma(\mathcal{R})$ for the positive and negative curvatures with the help of the cluster and void surface energies, respectively:

$$\sigma(\mathcal{R}) = \sigma^{c}(\mathcal{R}) \qquad \mathcal{R} > 0 \tag{14}$$

$$\sigma(\mathcal{R}) = \sigma^{v}(-\mathcal{R}) \qquad \mathcal{R} < 0. \tag{15}$$

The edge formation energy is then $\int \mathrm{d}A\sigma(\mathcal{R})$. We apply this first to a quarter space of stabilized jellium with a 90° edge and rounding radius r. The principal curvature radii are r and ∞ and therefore $\mathcal{R}^{-1} = \frac{1}{2}r^{-1}$. As a consequence, the formation energy of a rounded 90° edge per unit length is $\frac{1}{2}\pi r\sigma(2r)$. Correspondingly, the formation energy of the complementary 270° edge is $\frac{1}{2}\pi r\sigma(-2r)$. Then, $\frac{1}{2}\pi r\,[\sigma(2r) + \sigma(-2r) - 2\sigma]$ is the

curvature contribution to the cleavage energy of the bulk stabilized jellium into a quarter space and a three quarter space jellia with rounded edges.

A step on a surface is formed by a 90° edge and a 270° edge. The step formation energy per unit length is then

$$[(\pi - 4)r + h]\sigma + \tfrac{1}{2}\pi r\,[\sigma(2r) + \sigma(-2r) - 2\sigma] \tag{16}$$

where h is the height of the step. The first term in (16) is due to the increase of the surface area and the second term is a curvature correction. As an example, we consider a monolayer step on the Al(111) surface. Its height $h = a/\sqrt{3}$, where a is the FCC lattice constant. Then, using the maximum rounding $r = h/2$ ($< r_0$) and the data from table 3, the step formation energy per unit length is $40\,\mathrm{meV}\,a_B^{-1}$. In this case the curvature correction is less than $1\,\mathrm{meV}\,a_B^{-1}$. On the other hand, if we use for $\sigma(2r)$ the value of $26\,\mathrm{meV}\,a_B^{-2}$ (instead of $21\,\mathrm{meV}\,a_B^{-2}$) estimated from the self-consistent calculations for stabilized jellium spheres with $N = 3 \cdots 10$, the resulting step energy is $57\,\mathrm{meV}\,a_B^{-1}$. These two estimates bracket the result of $45\,\mathrm{meV}\,a_B^{-1}$ obtained by Scheffler and co-workers [7] with first-principles calculations (using a lattice constant corresponding to r_s slightly smaller than the 2.07 used here).

5. Conclusions

In conclusion, we have determined the formation energies of voids in stabilized jellium by calculating the self-consistent electron structures. The values of the planar surface energies and the curvature energies are obtained. Moreover, we have calculated the electronic structures and total energies of stabilized jellium spheres, mimicking small simple metal atom clusters. In this work we have considered different analytic expansions for the surface energies of spherical voids and clusters and determined the expansion coefficients. In principle, it is possible to extend the theory beyond the spherical shape in order to have a more realistic description of specific vacancy agglomerates or atomic clusters with facets, edges and corners. Also in these cases, analogously to the spherical case, the basis would be expansions in terms of characteristic dimensions of the void or the cluster, with well defined expansion coefficients.

In this work we have shown by self-consistent calculations that the stabilized jellium model gives physically meaningful results for the energetics of planar surfaces as well as of negatively or positively curved surfaces. In the case of alkali metals even the quantitative agreement with experiments is good. The generalized liquid drop model explains void formation energy data and it gives, apart from effects due to shell structure, a reasonable description for the total energies of small metal clusters.

Finally, our application to the formation energy of a step on the Al(111) surface demonstrates that simple models based on the stabilized jellium picture can provide insight into the structural properties of real surfaces.

Acknowledgments

We are grateful to J P Perdew for suggesting this study and for many helpful discussions, and M Scheffler for providing us with unpublished results. One of the authors (PZ) would like to thank the Laboratory of Physics at the Helsinki University of Technology and the Research Institute for Theoretical Physics at the University of Helsinki for their kind hospitality.

References

[1] Lang N D and Kohn W 1970 *Phys. Rev.* B **1** 4555
[2] Monnier R and Perdew J P 1978 *Phys. Rev.* B **17** 2595
[3] Lang N D 1983 *Theory of the Inhomogeneous Electron Gas* ed S Lundqvist and N H March (New York: Plenum) p 309
[4] Manninen M, Nieminen R M, Hautojärvi P and Arponen J 1975 *Phys. Rev.* B **12** 4012
[5] Nieminen R M 1978 *J. Nucl. Mater.* **69/70** 633
[6] Manninen M and Nieminen R M 1978 *J. Phys. F: Met. Phys.* **8** 2243
[7] Scheffler M, Neugebauer J and Stumpf R 1993 *J. Phys.: Condens. Matter* **5** 5A A91–4
[8] Häkkinen H, Merikoski J, Manninen M, Timonen J and Kaski K 1993 *Phys. Rev. Lett.* **70** 2451
[9] Perdew J P, Tran H Q and Smith E D 1990 *Phys. Rev.* B **42** 11627
[10] Shore H B and Rose J H 1991 *Phys. Rev. Lett.* **66** 2519
[11] Kiejna A 1993 *Phys. Rev.* B **47** 7361
[12] Fiolhais C and Perdew J P 1992 *Phys. Rev.* B **45** 6207
[13] Perdew J P, Ziesche P and Fiolhais C 1993 *Phys. Rev.* B **47** 16460
[14] Perdew J P, Wang Y and Engel E 1991 *Phys. Rev. Lett.* **66** 508
Makov G and Nitzan A 1993 *Phys. Rev.* B **47** 2301
[15] Perdew J P and Wang Y 1992 *Phys. Rev.* B **46** 12947
[16] Hinterman A and Manninen M 1983 *Phys. Rev.* B **27** 7262
Ekardt W 1984 *Phys. Rev.* B **29** 1558
Beck D E 1984 *Solid State Commun.* **49** 381
[17] Brajczewska M, Fiolhais C and Perdew J P 1993 *Int. J. Quantum Chem. S.* submitted
[18] Kittel C 1976 *Introduction to Solid State Physics* 5th edn (New York: Wiley)
[19] Ziesche P, Perdew J P and Fiolhais C 1993 unpublished
[20] Perdew J P 1993 private communication
[21] Tyson W R and Miller W A 1977 *Surf. Sci.* **62** 267